FOREX Publication
Open Access | Rapid and quality publishing

International Journal of
Electrical and Electronics Research (IJEER)
Research Article | Volume 12, Issue 4 | Pages 1142-1150 | e-ISSN: 2347-470X

Fast Charging System of Electric Vehicle Using Optimized Isolated Multi-Port DC-DC Converter based on Modified Coati Optimization Algorithm

Chithras Thangavel[1*] and Vinoth Krishnamoorthy[2]

[1]*Vel Tech Rangarajan Dr. Sagunthala R&D Institute of Science and Technology; chithras.gv@gmail.com*
[2]*Vel Tech Rangarajan Dr. Sagunthala R&D Institute of Science and Technology; vinothkrishna03@gmail.com*

***Correspondence:** Chithras Thangavel; chithras.gv@gmail.com

ABSTRACT- Once clean, renewable energy sources are used to charge the batteries in electric vehicles (EVs), the vehicles can produce zero gas emissions, greatly improving the environment. EVs and other distributed energy storage devices can be used in a smart microgrid to deliver energy to the loads throughout highest times, reducing the impact of load shading and improving the quality of the electricity. To achieve these goals of energy balance between EVs, the grid, and renewable energy sources, an isolated hybrid multiport converter is required. This paper develops an optimized isolated multi-port DC-DC converter for controlling power flow in multiple directions in an EV. This converter contains a dc-dc unidirectional converter, a bidirectional dc-dc converter, a triple active bridge (TAB), and a multi-port dual active bridge converter. Additionally, the Optimal Controller (OC) is developed to manage the power between the EV and the battery. The power flow is achieved by using the Modified Coati Optimization Algorithm (MCOA). In the MCOA, the optimal gain parameter of the converter is selected. In the planned technique, a bidirectional DC-DC converter can be considered to interconnect the EV battery towards deliver bidirectional power flow ability with the battery. The proposed approach is executed in MATLAB, and presentations are assessed by considering performance measures. Moreover, it is contrasted with the traditional approaches of particle swarm optimization (PSO) and grey wolf optimization (GWO).

Keywords: Triple active bridge, Modified coati optimization algorithm, bidirectional DC-DC converter, electric vehicle, and battery.

ARTICLE INFORMATION

Author(s): Chithras Thangavel and Vinoth Krishnamoorthy;
Received: 17/07/2024; **Accepted**: 26/09/2024; **Published**: 15/10/2024;
e-ISSN: 2347-470X;
Paper Id: IJEER 1707-28;
Citation: 10.37391/ijeer.120404
Webpage-link:
https://ijeer.forexjournal.co.in/archive/volume-12/ijeer-120404.html

1. INTRODUCTION

Over the past two decades, EVs have garnered significant attention and increased in popularity globally as a highly talented other towards decrease greenhouse gas discharges in the transport sector [1]. Furthermore, new economic research indicates that electric vehicles (EVs) will soon completely replace internal combustion engine (ICEV) vehicles. This makes it necessary to build charging stations all over the world that can handle the demands for the substantial quantity of electricity required to charge these EVs. However, there becomes a problem with the infrastructure for charging EVs as the number of vehicles on the road develops [2]. Charging these vehicles using the current electric grid may become more challenging and may not be the best course of action. Consequently, there is an increasing need to create an EV charging infrastructure that is reliable [3], sustainable, and powered by renewable energy sources. Decreasing the burden on the traditional power grid and promoting a cleaner, more maintainable transport industry are just two advantages of switching to grid-based charging solutions [4,5].

Researchers studying power electronic interfaces for electric vehicle systems have published a wide range of papers in the literature [6]. We address various topologies of isolated multi-port converters that are derived from multi-port converters. An isolated multi-port converter's conversion efficiency can be increased by applying the interleaving idea [7]. The output power of a multi-port energy converter is managed and regulated by the use of a single-leg active switching parameter. In the EV mentioned above, a dc/DC converter structure has been developed to analysis the energy transfer amid the battery and grid supply. This converter's switch count is dependent on the quantity of battery modules it contains [8]. For example, if there are 'n' battery designs, the architecture needs '2n' switches to function properly. An MCOA-based energy management technique has been suggested for efficient power management amid the grid source and battery as well as to overpower problems like overcharging of the grid source and excessive battery current during peak power [9]. This paper's primary contribution is outlined as follows:

This paper develops an optimized isolated multi-port DC-DC converter for controlling power flow in multiple directions in an EV. This converter contains a DC-DC unidirectional converter, a bidirectional DC-DC converter, TAB, and a multi-port dual active bridge converter.

FOREX Publication
Open Access | Rapid and quality publishing
International Journal of Electrical and Electronics Research (IJEER)
Research Article | Volume 12, Issue 4 | Pages 1142-1150 | e-ISSN: 2347-470X

Additionally, the OC is developed to manage the power between the EV and the battery. The power flow is achieved by using the MCOA. In the MCOA, the optimal gain parameter of the converter is selected. In the planned technique, a bidirectional DC-DC converter can be considered to interconnect the EV battery towards deliver bidirectional power flow ability with the battery.

The structure of the article's remaining part is as follows: The system's architecture and overview are described in *section 2*. The section on controller design is found in *section 3*. *Section 4 and 5* presents the conclusions of the paper as well as the simulated outcomes.

1.1. Related works

There are many linear controllers in the literature, such as H infinity controllers, proportional-resonant (PR) controllers, and proportional-integral (PI) controllers. There has also been discussion in the literature regarding the advancement of controllers based on soft computing.

Stochastic dynamic programming-based power management for ZEZ drive readiness has been proposed by Jemin Woo et al. [10]. Its goal is to maximize HEV charging efficiency. Using future probability information up to an unlimited time horizon, stochastic dynamic programming uses a Markov chain to simulate the driver's intentions and creates optimal controllers. Effective charging is further made possible by the suggested controller's consideration of the distance to the zero-emission zone. Up to around 21% more fuel efficiency is achieved using the proposed power management method when compared to stochastic dynamic programming solutions that do not account for the remaining distance.

Vinoth Kumar Manickam et al. [11] have presented a methodical methodology for managing power generators, electric car chargers, and battery chargers as a backup power source for electrical systems. This is made possible by accepting electric vehicles (EVs) as a useful element that possess the ability to store, use, and generate energy. With the help of this feature, which enables the charger to operate in Grid-to-vehicle (G2V) and V2G modes at any power factor, the electric vehicle (EV) can perform a variety of grid support tasks in addition to charging, such as voltage control, RPC, and THD reduction. The Assailant Inspired Chimp Optimization Algorithm (AIChOa) is a novel method that maximizes the gain of the PI controller by applying the ideas of voltage synchronization, RPC, and THD reduction.

Teja Barker et al. [12] have presented a carefully thought-out charging station design that works in unison with precision to optimize EV charging dynamics and Neural network-based grid management. This is achieved by using Adaptive Neuro-Fuzzy Inference System (ANFIS) technology for voltage-controlled Maximum Power Point Tracking (MPPT) in conjunction with Type 3 and 2 controllers.

To accommodate energy storage units (ESUs) and electric vehicles (EVs) across various power generation and demand scenarios, an adaptive sliding mode controller has been devised by R.S. Bajpai et al. [13]. By using a decentralized approach, the suggested adaptive sliding mode controller manages power distribution between the microgrid DC-link EVs and the ESUs. To confirm the sliding mode controller's effectiveness in battery charging applications, a thorough comparison between fuzzy logic and adaptive sliding mode control is conducted.

2. METHODS

Energy scarcity and environmental deterioration have garnered more attention in the past few years. The pollution caused by car exhaust emissions has increased with more people owning cars, which has forced an acceleration of the energy transition in automotive energy. Conventional EV energy storage systems are battery-powered storage devices with several drawbacks and shortcomings. At first, while an EV is rising or accelerating, its battery's power density is insufficient to fulfil its peak power requirement. Furthermore, the EV load will significantly increase as the power requirement is offset by adding more battery cells. To control power flow, this study proposes an optimized isolated multi-port DC-DC converter and an ideal charging and discharging controller for EVs to create a rapid charging system. In *figure 1*, the entire architecture of the suggested methodology is displayed.

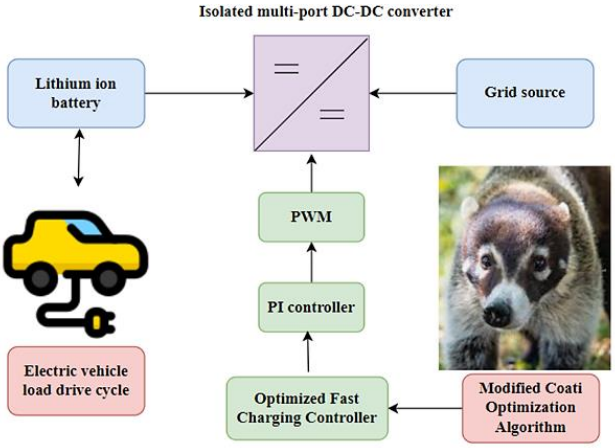

Figure 1. Architecture of the proposed model

The fast-charging system, which enhances the charging and discharging processes, provides the battery with maintenance. Furthermore, the battery is coupled with the grid to supply the necessary energy if the battery can be unable to sustain the load of electric vehicle. This is achieved by designing the controller-assisted optimized isolated multi-port DC-DC converter. Power management control's primary function is to balance out load demand by taking into account the battery's charging and discharging controller, which is determined by MCOA. The suggested strategy to extend battery life is energy management and charging using a discharge controller, which lowers the risk of overcharging and drying up the battery. There are two ways to use the grid to improve the battery. The grid is used in condition 1 to charge the battery when it is empty and to store extra energy when the battery is overcharged. The system model and system modelling are shown in the parts below.

FOREX Publication
Open Access | Rapid and quality publishing
International Journal of Electrical and Electronics Research (IJEER)
Research Article | Volume 12, Issue 4 | Pages 1142-1150 | e-ISSN: 2347-470X

3. THEORY AND CALCULATION

3.1 Modelling of Electrical Vehicle

When driving at different speeds, an EV needs a certain amount of energy to accelerate and brake. The amount of energy consumed by the EV depends on the energy requirements of the vehicle. In addition, the rolling friction force and aerodynamic resistance can exert their respective forces on a moving vehicle. Forces in an EV are related to several different things, including tire pressure [14], vehicle shape, pavement type, tire width and frontal surface. The vehicle is experiencing a resultant force that causes a velocity change that is connected to the instantaneous velocity under consideration and is reasonably easy to compute. Following that, driving force is typically used to calculate a vehicle's energy demand (DF). Furthermore, the difference in rolling resistance (RR), resultant force (RF), and aerodynamic resistance (AR) is what is referred to as the EVs.

$$DF = RF - AR - RR \tag{1}$$

The following formula is used to get the EV's RR:

$$RR = MGF_{to}(1 + kv^2) \tag{2}$$

Here, F_{to} is a low-speed resistance coefficient, G is the standard gravity acceleration, V is the vehicle speed, M is a vehicle mass, k is the rolling resistance coefficient. After the drag racing test is validated, the low-speed coefficient is computed and expressed as follows:

$$F_{to} = \frac{vb^2}{2gs_t} \tag{3}$$

Here, v_b is the initial speed of the vehicle and s_t Is a rolling distance of the vehicle. The low speed with RR coefficient for an EV traveling normally on the road is seen as falling between 0012 and 0014.

$$AR = \frac{1}{2}\rho c_x a v_r^2 \tag{4}$$

$$e = \frac{DFs}{\eta} \tag{5}$$

$$p = \frac{DFv}{\eta} \;\; or \;\; P = \frac{e}{T} \tag{6}$$

Here, ρ is an air density, c_x is a longitudinal direction through an air resistance coefficient correlated to vehicle shapes then ranges, A is defined as a vehicle coefficient of frontal superficial location, v_r^2 is the vehicle speed correlated to the air. The thermal resistance parameter, the car's instantaneous velocity, and the assumed drive architecture efficiency within the specified stage are used to calculate the EV's driving force together with the energy and instantaneous power needed to specify route *S* in a specific amount of time.

3.2. Modelling of Battery

Because of their life cycle, batteries connected to lithium-ion technology are frequently used in EVs. For lithium-ion battery simulation, the internal resistance model is taken into consideration because of its simple and accurate information representation. The battery's internal resistance model comprises an ideal cell with an internal resistance and an internal resistance with a series cell [15]. Whether the battery is charging or draining affects its internal resistance. The formula for the battery current, terminal voltage and output power is as follows:

$$P_B = V_{OC} I_B - R_{IN} I_B^2 \tag{7}$$

$$I_B = \frac{V_{OC} - \sqrt{{V_{OC}}^2 - 4P_B R_{IN}}}{2R_{IN}} \tag{8}$$

$$V_B = V_{OC} - R_{IN} I_B \tag{9}$$

$$V_B = \frac{V_{OC} - \sqrt{{V_{OC}}^2 - 4P_B R_{IN}}}{2} \tag{10}$$

Here, V_{OC} is an open circuit voltage, R_{IN} is an internal resistance,$I_B$is a terminal current, V_B is a terminal voltage and P_B is a battery output power. Calculating the quantity of charge that remains in the battery for use allows one to estimate the amount of energy that is saved. The state of charge (SOC) of a battery is its volume of accessible charge at its maximum charge capacity. Charging loss is quantified using the coulombic efficiency. The battery's SOC during charging and draining is represented by the following dynamic equation:

$$\mathrm{SOC} = \begin{cases} -\dfrac{\mathrm{I_B}}{\mathrm{c_{ah}}} & \mathrm{I_B} \geq 0 \\ -\dfrac{\mathrm{c_{eff} I_B}}{\mathrm{c_{ah}}} & \mathrm{I_B} < 0 \end{cases} \tag{11}$$

Here, c_{eff} is the Coulombic efficiency, T_B is a battery temperature and c_{ah} is the maximum capacity of a battery.

3.3. Modelling of isolated multi-port DC-DC converter

A triple active bridge, a generic multiport dual active bridge, a DC-DC unidirectional converter, and a bidirectional DC-DC converter are all combined in this section to provide the converter's full functioning mode. In *figure 2*, the converter diagram is displayed.

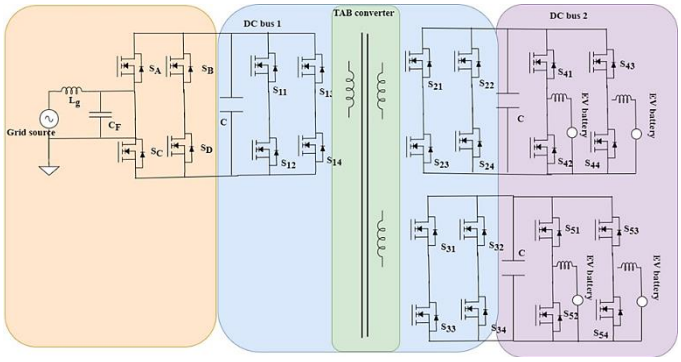

Figure 2. Isolated multi-port DC-DC converter

FOREX Publication
Open Access | Rapid and quality publishing
International Journal of Electrical and Electronics Research (IJEER)
Research Article | Volume 12, Issue 4 | Pages 1142-1150 | e-ISSN: 2347-470X

To facilitate bidirectional power flow, the recommended approach considers utilizing a bidirectional DC-DC converter to interface the EV battery with the utility grid and energy storage. For the battery interface, a traditional dc-dc boost converter is also considered. The electric car loads receive the energy that comes from the battery sources. To facilitate bidirectional power flow with the utility grid, a bidirectional AC-DC converter is used to generate sinusoidal DC on the grid side for high-quality power conversion. This technique communicates with the battery storage, which controls the charging and discharging operations of the battery, using a bidirectional DC-DC converter. To accommodate a variety of DC voltage sources, the proposed approach is further expanded to several DC busses using a multi-winding transformer.

3.4. Modified Coati Optimization Algorithm

This optimization algorithm is developed to select the optimal gain parameters of the converters. This MCOA is a combination of COA and a chaotic map. It is a member of the Nasuella genus and Nasua of the Procyonidae family are referred to as coatis, also known as coatimundis. Native to the southwest region of the United States, South America, Central America, and Mexico, it is a diurnal animal [16]. The coatis' method of attacking iguanas and their traits for fending off predators are both effective defensive mechanisms. The general concept for creating the suggested COA approach came from the process of generating these natural coati's traits. As population members of this algorithm, the coatis are defined in the context of the COA approach, a population-related metaheuristic.

Step 1*: *Initialization

In the initialization process, the random gain parameters are initialized. Each coati's position in the search space is used to calculate the parameters for the decision parameters. Therefore, the location defines a potential fix for the problem in the COA. The following equation is used to randomly set the search space location during the COA implementation initialization process:

$$T_I: T_{I,J} = LB_J + R.\left(UB_J - LB_J\right), \quad I = 1,2,\dots,N \;\; J = 1,2,\dots M \tag{12}$$

Here, UB_J is an upper bound, LB_J is a lower bound, R is a random real number in the range [0,1], M is the count of decision parameters, N is the count of coatis, $T_{I,J}$ is the parameter of the decision parameter and $T_I$is the location of the coati in the search space. The population matrix is the mathematical definition of the coati population of the COA

$$T = \begin{bmatrix} T_1 \\ \dots \\ T_I \\ \dots \\ T_N \end{bmatrix}_{N\times M} = \begin{bmatrix} T_{I,1} & \dots & T_{1,J} & \dots & T_{1,M} \\ \dots & \dots & \dots & \dots & \dots \\ T_{I,1} & \dots & T_{I,J} & \dots & T_{I,M} \\ \dots & \dots & \dots & \dots & \dots \\ T_{N,1} & \dots & T_{N,J} & \dots & T_{N,M} \end{bmatrix}_{N\times M} \tag{13}$$

The placement of potential solutions within the choice parameters enhances the calculation of different parameters for the issue's goal function. The parameter of the goal function in this method serves as a measure of a potential solution's quality.

Step 2: Fitness Function

In this algorithm, the best gain variables are chose related on the Integral Absolute Error (IAE). The fitness function is formulated as follows,

$$FF = MIN(IAE) \tag{14}$$

$$IAE = \int_0^\infty |E(T)|\, dt \tag{15}$$

$$E(T) = V_{ref} - V \tag{16}$$

Here, V_{ref} is a reference voltage and V is a voltage source. Thus, the ideal member of the population is the one who makes it possible to compute the optimal parameter for the objective function. Every time the algorithm iterates, the optimal member of the population is also upgraded because the candidate solutions are upgraded as well. The exploitation and exploration phases are the two stages that make up the coatis updating process.

Algorithm 1: *Pseudocode of the proposed methodology*

```
Initialize MCOA
Input of the random gain parameters of PI
Set the number of coatis and number of iterations
Initialization of the population of complete coatis
Compute the fitness function
For T=1:t
        Update the location of the iguana related on the chaotic mapseq (17)
        Exploration stage
        Compute new positionEq (18, 19)
        Upgrade position of coati
End for
        For I=1+[N/2]: N
        Compute the random location of the iguana
        Compute new location by eq (20,21)
        Update the position
End for
        Exploitation stage
        Compute the local bounds
        For I=1: N
        Compute new location by eq (22,23)
        Upgrade the position
        End for
Save the optimal candidate solution
End for
The output of best-achieved solution by MCOA
End MCOA
```

Step 3: Chaotic map

The definition of chaotic maps is discrete-time dynamical architectures. This strategy requires the long-period random number sequences to be in a specific spot in the COA [17]. This

FOREX Publication
Open Access | Rapid and quality publishing
International Journal of Electrical and Electronics Research (IJEER)
Research Article | Volume 12, Issue 4 | Pages 1142-1150 | e-ISSN: 2347-470X

algorithm computes the random variable while considering a chaotic map that is created while the program runs.

The formulation is as follows:
In the equation, $chaos(t)$ is utilized instead of the randomly assigned parameter and T is the present iteration of the algorithm.

Step 4: Exploration Stage: Iguana Hunting and Attacking Methods

The first step towards improving the coati population in the search space is to analyze their method of attacking iguanas. The capacity to move to different locations in the search space that characterizes the COA exploration capability in global search within the problem-solving space is provided by this technique to coatis. The COA design assumes that the iguana is located where the best member of the population is. Another theory holds that while some coatis climb the tree, others remain below to wait for the iguana to drop to the ground. As a result, the following mathematical formula represents the coati position growing from the tree:

$$T_I^{P1}: T_{I,J}^{P1} = T_{I,J} + R.\left(Iguana_J - I.T_{I,J}\right), \quad for\ I = 1,2,\dots,\left\lfloor\frac{N}{2}\right\rfloor\ \ and\ J = 1,2,\dots,M \qquad (17)$$

The iguana is found in an arbitrary spot inside the search area once it hits the ground. Concerning this arbitrary location, coats on the ground move in the search space, which is carried out by applying the equation below;

$$\text{Iguana}^{g}: \text{Iguana}_J^{g} = \text{LB}_J + \text{R}.\left(\text{UB}_J - \text{LB}_J\right), \quad J = 1,2,\dots,M \qquad (18)$$

$$\text{T}_I^{P1}: \text{T}_{I,J}^{P1} = \begin{cases} \text{T}_{I,J} + \text{R}.\left(\text{Iguana}_J^{g} - \text{i}.\,\text{T}_{I,J}\right) & \text{f}_{\text{iguana}^g} < \text{f}_i \\ \text{T}_{I,J} + \text{R}.\left(\text{T}_{I,J} - \text{Iguana}_J^{g}\right) & \text{Else} \end{cases} \qquad (19)$$

$$For\ I = \left\lfloor\frac{N}{2}\right\rfloor + 1, \left\lfloor\frac{N}{2}\right\rfloor + 2, \dots, N \quad and\ J = 1,2,\dots,M \qquad (20)$$

If each coati's new location improves the objective function's parameter, the updating process accepts it; if not, the coati stays in the original location. The algorithm is updated using the following formula:

$$\text{T}_I = \begin{cases} \text{T}_I^{P1} & \text{f}_I^{P1} < \text{f}_I \\ \text{T}_I & \text{Else} \end{cases} \qquad (21)$$

Where, $\lfloor . \rfloor$ is the floor function, f_{iguana^g} is the parameter of the objective function, $Iguana_J^g$ is the dimension, $Iguana^g$ is the location of the iguana on the ground, it is randomly created, I is an integer that is randomly created, $iguana$ is a iguana position in the search space that normally defines the location of the optimal member, R is the random number in the interval, f_I^{P1} is an objective function, $T_{I,J}^{P1}$ is a dimension and T_I^{P1} is a new location computed for the coati.

Step 5: The stage of exploitation: The act of running away from potential threats

Coatis' natural abilities to elude and outrun predators provide the basis for the second method of updating their position in the search space, which is mathematically constructed. A coati flees from its predation when it comes under attack. A random position is generated near the location of each coefficient associated with the following equations to imitate these features.

$$\text{LB}_J^{\text{LOCAL}} = \frac{\text{LB}_J}{\text{T}}, \text{UB}_J^{\text{LOCAL}} = \frac{\text{UB}_J}{\text{T}}, \text{where T} = 1,2,\dots,\text{t} \qquad (22)$$

$$\text{T}_I^{\text{P2}}: \text{T}_{\text{I,J}}^{\text{P2}} = \text{T}_{\text{I,J}} + (1 - 2\text{R}).\left(\text{LB}_J^{\text{LOCAL}} + \text{R}.\left(\text{UB}_J^{\text{LOCAL}} - \text{LB}_J^{\text{LOCAL}}\right)\right) \quad \text{I} = 1,2,..\,\text{N}, \quad \text{J} = 1,2,\dots,\text{M} \qquad (23)$$

If the newly computed position increases the objective function's parameter, then it is acceptable. This scenario is calculated using the formula shown below.

$$\text{T}_\text{I} = \begin{cases} \text{T}_\text{I}^{\text{P2}} & \text{f}_\text{I}^{\text{P2}} < \text{f}_\text{I} \\ \text{T}_\text{I} & \text{Else} \end{cases} \qquad (24)$$

Where, UB_J^{LOCAL} is a local upper bound of the decision variable, LB_J^{LOCAL} is a local lower bound of the decision, R is a random number in the interval, f_I^{P2} is the objective function value, $T_{I,J}^{P2}$ is the dimension and T_I^{P2} is the new location computed for the coati related to the second phase of COA. In this algorithm, the optimal gain parameters of the converter are achieved. After that, it is sent to the converter and managed the battery management by the charging and discharging procedure.

4. RESULTS AND DISCUSSIONS

The performance of the suggested approach is examined and verified in this section. The suggested approach was created to strengthen the EV battery's quick charging mechanism. By considering the suggested rapid charging controller, this suggested methodology extends battery life. The rapid charging controller is used to manage the battery to extend its life. This controller allows for appropriate EV load demand adaptation during charging and discharging. Performance analysis and comparison are used to assess the suggested method's implementation in MATLAB. The design parameter assumption is used to validate the proposed method's comparison. The battery and the suggested controller performance computation are validated by taking into account the EV load. Design the EV with controller parameters are listed in *table 1*.

Table 1. Simulation Parameters

S. No	Description	Parameters
1	Open circuit voltage	2.92V
2	Terminal resistance	0.064 Ohm
3	Vector of state of charge values	0,0. 01,...,1
4	Cell capacity	2.735H/A
5	Initial temperature	25
6	Battery initial	0.8
7	Iterations	100
8	Initial population	50
9	Upper bound	-10
10	Lower bound	10

FOREX Publication
Open Access | Rapid and quality publishing
International Journal of Electrical and Electronics Research (IJEER)
Research Article | Volume 12, Issue 4 | Pages 1142-1150 | e-ISSN: 2347-470X

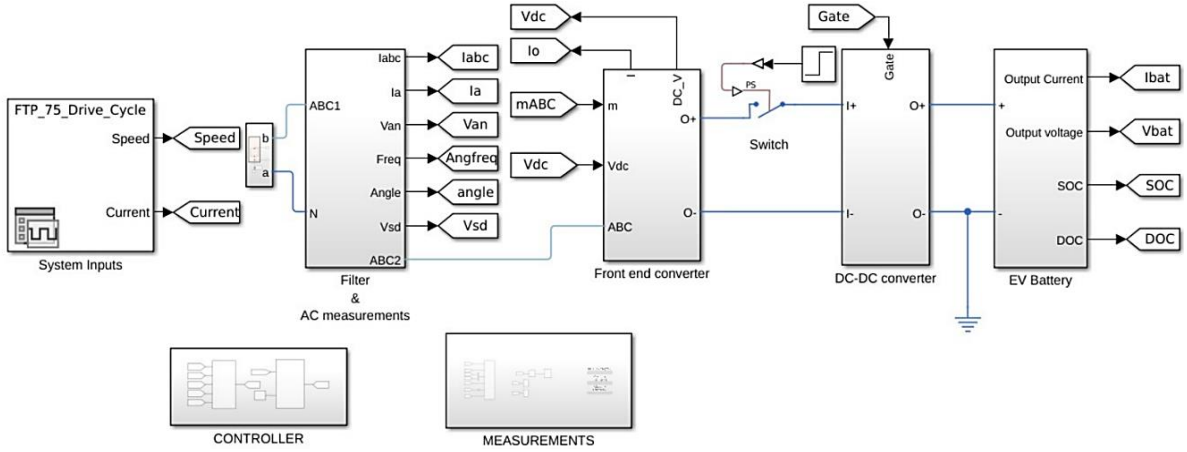

Figure 3. Simulink diagram

Figure 3 displays the suggested methodology's Simulink diagram. The EV is first built with speed-related load conditions. Energy is used, and the battery is charged and discharged following the vehicle load.

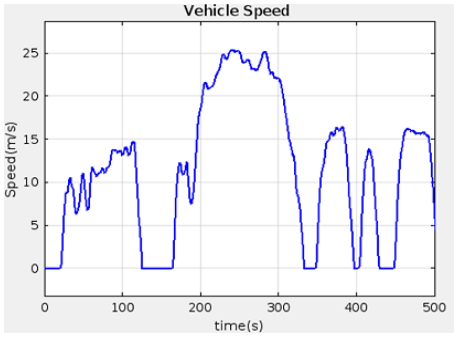

(a)

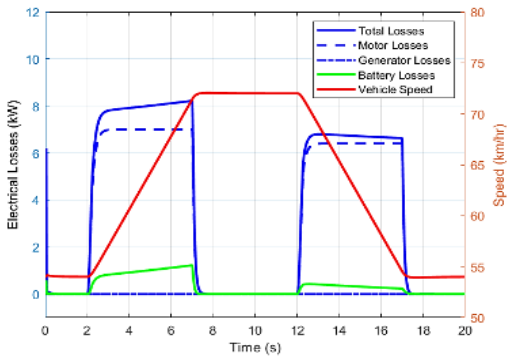

(b)

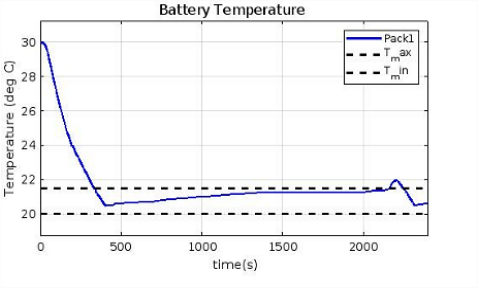

(c)

Figure 4. (a) Vehicle Speed, (b) Vehicle Speed with electrical losses and (c) Battery temperature

Figure 4(a) presents the analysis and speed of the EV. In connection with this procedure, the speed varies between 5 and 25 m/s. Increasing the speed of an electric vehicle results in higher energy consumption when the energy is drawn from the battery. Similarly, because the energy comes from the battery, the EV's speed is reduced and its energy usage is minimal. Using battery energy storage devices, the load is compensated based on this process. In the process of compensating for the load requirement, the battery continues to charge and discharge. The EV's battery problems and shorter battery life are caused by this process. A quick charging controller was created to improve the performance of batteries. There are various types of losses associated with an electric vehicle load, including electrical losses from batteries, generators, motors, and total losses. The speed of the car caused this loss. *Figure 4(b)* illustrates this scenario.

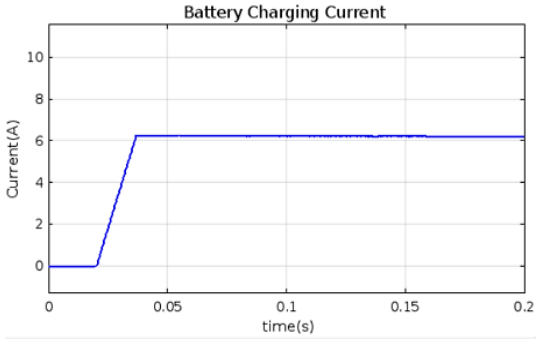

(a)

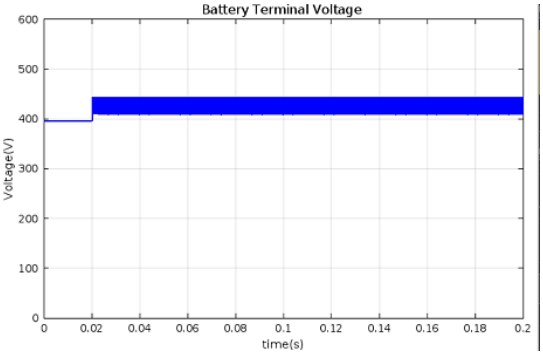

(b)

FOREX Publication
Open Access | Rapid and quality publishing
International Journal of Electrical and Electronics Research (IJEER)
Research Article | Volume 12, Issue 4 | Pages 1142-1150 | e-ISSN: 2347-470X

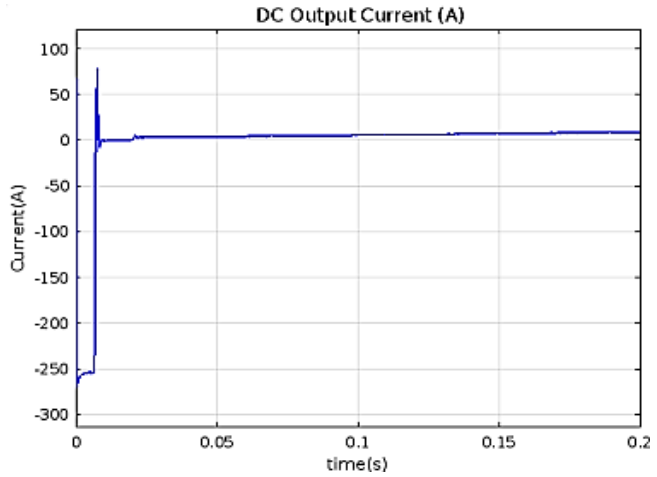

(c)

Figure 5. (a) Battery current, (b) Battery voltage and (c) DC output current

Figures 4(c) and *figure 5(a)* display the temperature and charging current of the battery. The battery's temperature is 30^0C; its minimum and maximum are 21^0C and 20^0C, respectively. The process of charging and draining a battery affects its temperature. The process of charging and discharging the battery affected the charging current as well. The battery charging current in question has a maximum of 2A and a minimum of 6A. During the load balancing process, the battery terminal voltage, which is 450V, oscillates to 410V. The process in question facilitates the management of batteries and loads for electric vehicles.

By utilizing the battery and voltage source, an EV can achieve load correction. To the isolated multi-port converter, these inputs are connected. Measured and shown in *figures 5(b)* and (c). This DC output current to input current converter. 50A is the greatest current that can flow, and 22A is the minimum. The EV's needed power and load requirements are interfaced with this converter. The converter current is also adjusted following the electric vehicle's load demand.

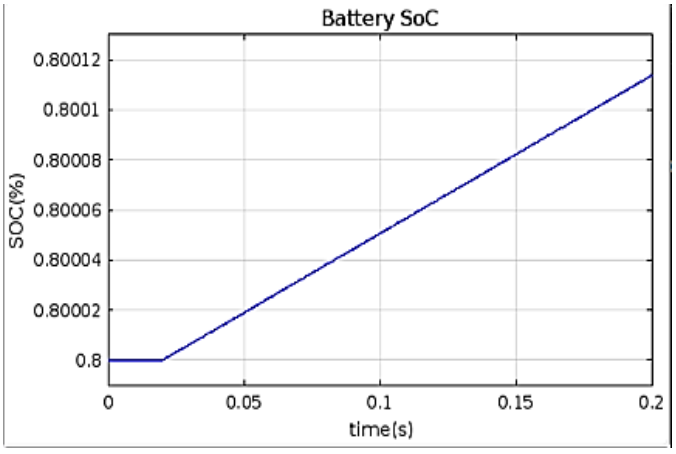

(a)

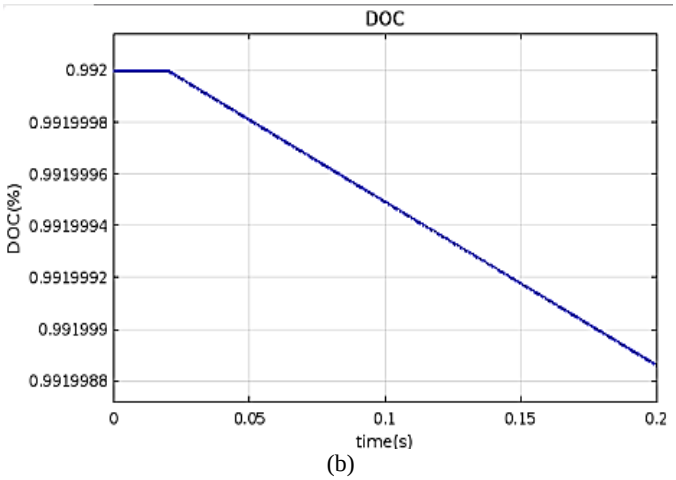

(b)

Figure 6. (a) Analysis of SOC, (b) Analysis of DOC

When adjusting for EV load requirements, the battery's condition is calculated using the SOC and DOC metrics. The ideal SOC and DOC values are 0.8 and 0.9, respectively. *Figures 6(a)* and *6(b)* depict the SOC and DOC, respectively. The process of charging and discharging results in changes to the SOC and DOC. The intended controller was created to control the SOC and DOC conditions while staying within the parameters. We can infer from this study that the suggested controller has always attained the best SOC and DOC conditions whenever an EV occurs. The EV's life cycles are improved and the battery's lifespan is extended with this control over SOC and DOC. Ultimately, the suggested controller optimizes the management of the EV load and improves battery lifecycles. Evaluating the best pulses to use with the isolated multi-port converter improves these procedures.

With the MCOA in mind, the converter's pulses are tuned. The IAE is taken into consideration as this optimization procedure moves forward. It is calculated taking the EV system's voltage differential into account. The fitness evaluation considers the fluctuations to identify the appropriate gain parameters of the PI. *Figure 7* displays the convergence analysis of the optimization procedure.

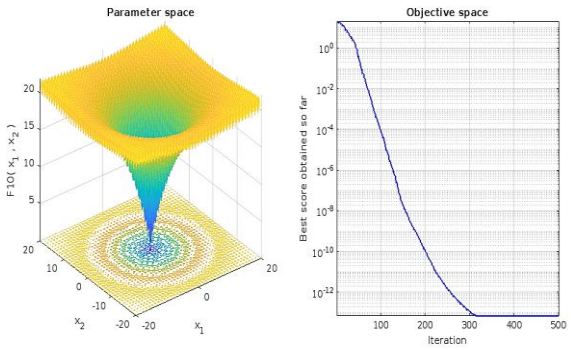

Figure 7. Convergence Analysis

FOREX Publication
Open Access | Rapid and quality publishing
International Journal of Electrical and Electronics Research (IJEER)
Research Article | Volume 12, Issue 4 | Pages 1142-1150 | e-ISSN: 2347-470X

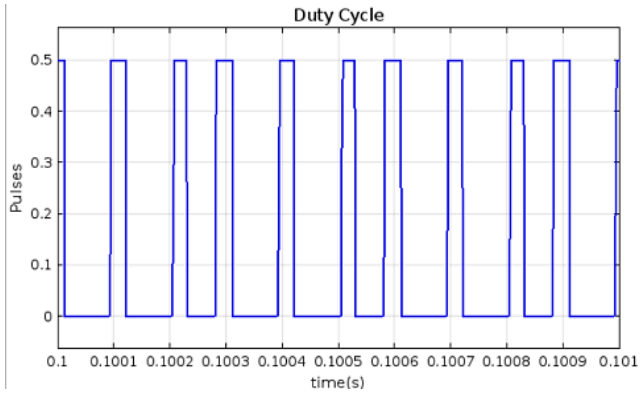

(a)

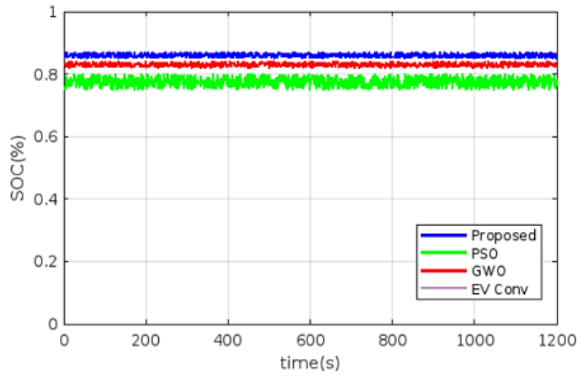

(b)

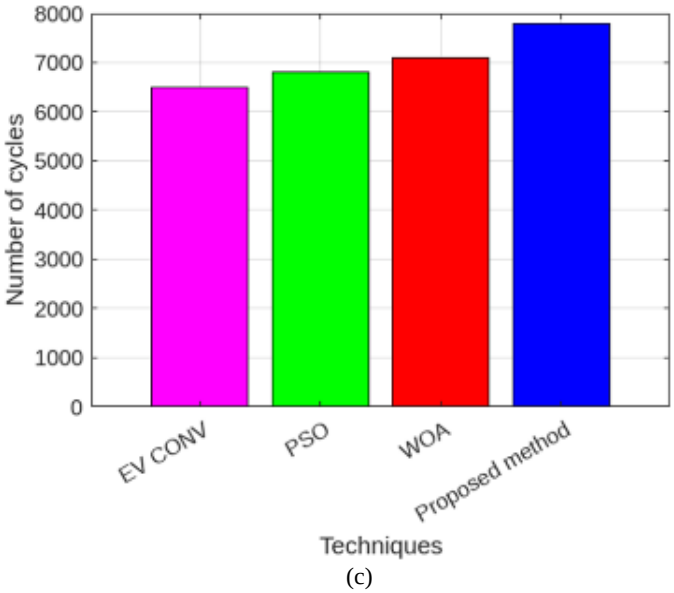

(c)

Figure 8. (a) Switching pulses, (b) Comparison of SOC and (c) Number of cycles

The best gain parameters are chosen in this convergence study after 300 iterations, altering the converter's pulses and improving the performance of the suggested architecture. In an EV, this gain parameter improves battery performance. In *figure 8(a)*, the generated pulses are shown. Switching pulses alter the isolated multi-port converter's operation, improving the EV process.

Table 2. Number of cycles

S. No.	Methods	Number of cycles
1	Proposed	7800
2	WOA	7000
3	PSO	6800
4	EV conv	6200

The proposed approach is examined using the SOC to validate it. *Figure 8(b)* analyses and displays the SOC comparison. A comparison is made between the suggested approach and traditional methods like PSO, GWO, and EVCON. While traditional methods get SOCs of 0.81, 0.80, and 0.79, the suggested method achieves SOC of 0.82. Through the course of the charging and discharging procedures, the suggested methodology achieves ideal SOC in this validation. The proposed approach is examined using the number of cycles to validate it. Figure 8(c) and Table 2 analyses and displays the number of cycle's comparison. A comparison is made between the suggested approach and traditional methods like PSO, GWO, and EVCON. While traditional methods get several cycles of 7000, 6800, and 6200, the suggested method achieves several cycles of 7800. Through the course of the charging and discharging procedures, the suggested methodology achieves a high number of cycles in this validation.

5. CONCLUSION

An EV's power flow can be adjusted in several directions with the help of the optimized, isolated multi-port DC-DC converter in this research. Triple active bridge (TAB), bidirectional dc-dc, multi-port dual active bridge, and unidirectional dc-dc converters are all included in this converter. The power management between the battery and the EV is another function for which the OC was designed. With the aid of the MCOA, the power flow has been produced. The MCOA has chosen the converter's ideal gain parameter. In the suggested method, an EV battery is interfaced with a bidirectional DC-DC converter to enable bidirectional power flow capability. Performance metrics are taken into consideration when evaluating the suggested method, which has been implemented in MATLAB. Furthermore, a comparison has been made with the traditional methods of PSO and GWO. By considering the battery lifecycles, the suggested methodology has been assessed. In comparison to traditional methods, it has attained a long battery life (7800 cycles). The best methodology will be used to examine and assess real-time evaluation in the future.

REFERENCES

[1] S. S. G. Acharige, M. E. Haque, M. T. Arif, N. Hosseinzadeh, K. N. Hasan and A. M. T. Oo, "Review of Electric Vehicle Charging Technologies, Standards, Architectures, and Converter Configurations," in IEEE Access, vol. 11, pp. 41218-41255, 2023, doi: 10.1109/ACCESS.2023.3267164.

[2] Karneddi, Harish, and Deepak Ronanki. "Reconfigurable Battery Charger with a Wide Voltage Range for Universal Electric Vehicle Charging Applications." IEEE Transactions on Power Electronics, vol. 38, no. 9, Sep. 2023, pp. 10606-10610. https://doi.org/10.1109/tpel.2023.3289394.

[3] Mateen, Suwaiba & Amir, Mohammad & Haque, Ahteshamul & Bakhsh, Farhad. (2023). Ultra-fast charging of electric vehicles: A review of power

FOREX Publication
Open Access | Rapid and quality publishing

International Journal of Electrical and Electronics Research (IJEER)
Research Article | Volume 12, Issue 4 | Pages 1142-1150 | e-ISSN: 2347-470X

electronics converter, grid stability and optimal battery consideration in multi-energy systems. Sustainable Energy, Grids and Networks. 35. 101112. 10.1016/j.segan.2023.101112.

[4] Saha, Jaydeep & Kumar, Nishant & Panda, Sanjib. (2023). Adaptive Grid-Supportive Control for Solar-Power Integrated Electric-Vehicle Fast Charging Station. IEEE Transactions on Energy Conversion. PP. 1-11. 10.1109/TEC.2023.3260191.

[5] Ramesh Jatoth and B. Mangu (2023), Grid-Tied Solar Power Sharing with V2G and G2V Power Exchange with Dual Bridge Integrated Electrical Vehicle. IJEER 11(1), 192-201. DOI: 10.37391/IJEER.110127.

[6] Varun krishna paravasthu, Balasubbareddy Mallala and B. Mangu (2024), An Enhanced Multi-Objective Evolutionary Optimization Algorithm based on Decomposition for Optimal Placement of Distributed Generation and EV Fast Charging Stations in Distribution System. IJEER 12(2), 575-580. DOI: 10.37391/IJEER-120232.

[7] Karmaker, Ashish & Hossain, Md. Alamgir & Pota, Hemanshu & Onen, Ahmet & Jung, Jaesung. (2023). Energy Management System for Hybrid Renewable Energy-Based Electric Vehicle Charging Station. IEEE Access. PP. 1-1. 10.1109/ACCESS.2023.3259232.

[8] Assadi, Seyed & Gong, Zhe & Coelho, Nathan & Zaman, Mohammad & Trescases, Olivier. (2023). Modular Multi-Port Electric-Vehicle DC Fast-Charge Station Assisted by a Dynamically Reconfigurable Stationary Battery. IEEE Transactions on Power Electronics. PP. 1-12. 10.1109/TPEL.2023.3237622.

[9] Zanatta, Nicola et al. “A Two-Stage DC-DC Isolated Converter for Battery-Charging Applications.” IEEE Open Journal of Power Electronics 4 (2023): 343-356.

[10] Woo, Jemin & Han, Seohee & Ahn, Changsun. (2024). SDP-Based Battery Charging Controller for Hybrid Electric Vehicles in Preparation for Zero-Emission Zone Drives. International Journal of Precision Engineering and Manufacturing-Green Technology. 10.1007/s40684-024-00609-9.
[11] Manickam, Vinoth Kumar, and K. Dhayalini. "Hybrid optimized control of bidirectional off-board electric vehicle battery charger integrated with vehicle-to-grid." Journal of Energy Storage 86 (2024): 111008.

[12] Barker, Teja, Arnab Ghosh, Chiranjit Sain, Furkan Ahmad, and Luluwah Al-Fagih. "Efficient ANFIS-driven power extraction and control strategies for PV-bess integrated electric vehicle charging station." Renewable Energy Focus 48 (2024): 100523.

[13] Bajpai, R. S., Apoorva Srivastava, Amarjeet Singh, and Shailesh Kumar. "Intelligent Control of DC Microgrid Involving Multiple Renewables for Fast Charging Control of Electric Vehicles." Electric Power Components and Systems (2024): 1-22.

[14] Saha, Jaydeep, Nishant Kumar, and Sanjib Kumar Panda. "Adaptive grid-supportive control for solar-power integrated electric-vehicle fast charging station." IEEE Transactions on Energy Conversion 38, no. 3 (2023): 2034-2044.

[15] Hu, Qiuhao, Mohammad Reza Amini, Ashley Wiese, Julia Buckland Seeds, Ilya Kolmanovsky, and Jing Sun. "Electric vehicle enhanced fast charging enabled by battery thermal management and model predictive control." IFAC-PapersOnLine 56, no. 2 (2023): 10684-10689.

[16] Dehghani, Mohammad, Zeinab Montazeri, Eva Trojovská, and Pavel Trojovský. "Coati Optimization Algorithm: A new bio-inspired metaheuristic algorithm for solving optimization problems." Knowledge-Based Systems 259 (2023): 110011.Hashim, Fatma A., Essam H. Houssein, Reham R. Mostafa, Abdelazim G. Hussien, and Fatma Helmy. "An efficient adaptive-mutated coati optimization algorithm for feature selection and global optimization." Alexandria Engineering Journal 85 (2023): 29-48.

[17] Chakravarthy, Sannasi, Bharanidharan Nagarajan, V. Vinoth Kumar, T. R. Mahesh, R. Sivakami, and Jonnakuti Rajkumar Annand. "Breast tumor classification with enhanced transfer learning features and selection using chaotic map-based optimization." International Journal of Computational Intelligence Systems 17, no. 1 (2024).